Explor Anim Med Res.
Vol. 14, Issue 1, 2024
DOI: 10.52635/eamr/14.1.112-123

ISSN 2277-470X (Print), ISSN 2319-247X (Online)
Website: www.animalmedicalresearch.org

Research Article

HISTOARCHITECTURAL ANOMALIES INDUCED BY ANTIBIOTIC FLORFENICOL IN COMMERCIALLY IMPORTANT CATFISH *PANGASIANODON HYPOPHTHALMUS*

Nilemesh Das[1,2], Thangapalam Jawahar Abraham[2*], Asit Kumar Bera[1], Sanjib Kumar Manna[1], Arya Sen[2], Sohini Chatterjee[1]

Received 27 March 2024, revised 17 June 2024

ABSTRACT: Antibiotics are widely used to prevent and treat bacterial infections, increasing aquaculture productivity. However, their imprudent use can lead to unintended consequences, including pathological alterations in vital organs of aquatic organisms. The safety of florfenicol following in-feed administration at 10 times the recommended dose and three times the recommended period in *Pangasianodon hypophthalmus* was studied. Florfenicol induced significant histoarchitectural anomalies as observed from the photomicrographs of double-stained sections of various tissues, including gills, liver, and kidneys of *P. hypophthalmus*, following in-feed administration at graded doses, *viz.*, 0mg, 10mg, 30mg, 50mg and 100 mg/kg biomass^{-1} day^{-1} for 30 days, *i.e.*, three times the recommended therapeutic duration. Gills exhibited lamellar fusion, epithelial lifting, and hyperplasia indicative of respiratory distress. There were hepatocellular vacuolation, degeneration, and congestion, suggesting impaired hepatic integrity. The kidney sections demonstrated tubular degeneration, necrosis, and interstitial inflammation implying renal dysfunction. These changes were prominent at higher doses, mostly in 50 mg and 100 mg groups, and in the extended duration of the treatment, underscoring the potential adverse effects of florfenicol on the histological integrity and physiological homeostasis of *P. hypophthalmus*. As the catfish species holds significant economic value in Asian aquaculture, understanding the impacts of antibiotic exposure is crucial for sustainable fish farming practices. Implementing appropriate antibiotic usage protocols and monitoring strategies can mitigate the risks associated with antibiotic-induced pathological alterations in commercially important aquatic species.

Keywords: Florfenicol, Pangas, Histoarchitectural anomalies, Commercial aquaculture.

INTRODUCTION

Antimicrobials play a vital role in the aquaculture industry, aiding in the prevention and treatment of bacterial diseases and reducing biological loss. However, indiscriminate use of antibiotics poses significant threats to fish health and farm productivity [1]. Florfenicol (FFL), a broad-spectrum semi-synthetic antibiotic, has been widely employed in aquaculture practices, including in the farming of *Pangasianodon hypophthalmus*, (Sauvage, 1878), also called striped catfish. While effective in combating bacterial infections, the indiscriminate use of antibiotics raises concerns regarding its potential adverse effects on fish and the aquatic environment. Antibiotics have been receiving increasing attention regarding their potentially harmful environmental impact mainly because they induce biological effects and persist for a long time in the water, soil, and organisms [2]. The most critical

[1]*ICAR-Central Inland Fisheries Research Institute, Barrackpore, Kolkata - 700120, India.*
[2]*Department of Aquatic Animal Health, West Bengal University of Animal and Fishery Sciences, Chakgaria, Kolkata- 700094, India.*
Corresponding author. e-mail: abrahamtj1@gmail.com

aspect of assessing the safety of an antibiotic in aquaculture is understanding its impact on the histological integrity of various tissues of the target fish species. Histoarchitectural anomalies, encompassing structural abnormalities at the cellular and tissue levels, serve as sensitive indicators of the toxicity potential of a pharmaceutical agent [3]. In the context of *P. hypophthalmus*, the most cultured catfish in the world, a comprehensive investigation into the histological alterations triggered by FFL is essential for elucidating potential health risks and guiding the therapeutic and preventive use potential of FFL.

Previous studies indicated the toxicity potential of FFL in treated fish [4]. Understanding the nature and extent of FFL-induced tissue anomalies is imperative for evaluating the overall health status of fish populations subjected to antibiotic treatment and mitigating potential adverse consequences on animal welfare and food safety. While previous studies have investigated the histopathological effects of drugs including FFL in various fish species [3, 4], comprehensive assessments specific to *P. hypophthalmus* remain scarce. Given the economic significance of this species in global and particularly in Asian aquaculture production, approximately 2% of global aquaculture production and 40% of global catfish production [5], there is a pressing need for targeted research elucidating the histological responses of *P. hypophthalmus* to FFL administration. Such investigations are essential for developing an evidence-based therapeutic schedule and suitable management practices aiming to safeguard fish health and environmental sustainability within the aquaculture sector. In this study, we aimed to address this knowledge gap by conducting a systematic histopathological examination of FFL-induced histoarchitectural alterations in *P. hypophthalmus* that would provide valuable insights into the potential health risks associated with FFL usage and contribute to the development of targeted strategies for antibiotic stewardship and aquatic health management.

MATERIALS AND METHODS

The antibiotic florfenicol is recommended for the treatment of bacterial infections in finfish at 10 mg/kg biomass^{-1} day^{-1} for 10 consecutive days [6]. The safety of FFL in *P. hypophthalmus* was studied following in-feed administration at 10 times the recommended dose and three times the recommended period as per USFDA [6]. The experiment was repeated three times from March to November 2023. Institute Ethical guidelines were followed for the experiments (2167GO/RBi/S/22/CPCSEA).

Experimental design

The acclimatized fish, with an average body weight of 43.35±3.37 g, were divided into five groups, each group had three tanks with 40 numbers of fish in each tank. FFL (TCI, F0811) was administered at different doses, *viz.*, 10 mg kg^{-1} (1×), 30 mg kg^{-1} (3×), 50 mg kg^{-1} (5×) and 100 mg kg^{-1} (10×) biomass^{-1} day^{-1} through the prepared (top-dressed) medicated feed daily for 30 days. A binder was prepared with 5% sago pearls, *i.e.*, 5 g of sago pearls in 100 mL of water, soaked overnight, and heated till the solution turned turbid and filtered. The calculated amount of FFL, with the assigned concentrations, as per the live weight of fish in each tank was dissolved in the above binder and smeared uniformly over the pre-weighed floating feed pellets (32% crude protein, and 5% crude fat, 1.2 mm grain size), mixed and air dried in a hot air oven at 40°C for one hour. After 30 days of feeding, the total water in every tank was replaced to remove the drug residue in the fish environment and fish were offered basal feed for another 10 days. The control group of fish received feed without antibiotics but with the binder throughout the experiment. Three fish from each tank were randomly netted, humanely euthanized using clove oil at 100 µg L^{-1} in water), weighed, and dissected.

Sample collection

The treated and control groups' gill, kidney, liver, and spleen samples were collected from each tank on days 0, 10, 20, and 30 of FFL dosing, and day 40 (*i.e.*, day 10 post-FFL-dosing) for histopathology. The collected tissue samples from *P. hypophthalmus* were fixed in Bouin's fixative for 24 hours. The tissues were placed in 70% ethyl alcohol after fixation and left overnight. The histological analysis was performed following Robert's [7] description.

Tissue processing, embedding sectioning, and photomicrography

Small bits of different 'fixed' tissues were removed from the 70% ethyl alcohol and were dipped in a series of ethyl alcohol solutions with increasing concentrations (85%, 90%, and 100%) to dehydrate. The tissues were dipped in each alcoholic concentration for 90 min with two changes. The tissues were placed in xylene following dehydration to make them translucent. Once the tissue was submerged in liquid

paraffin for at least 150 min, the paraffin was allowed to permeate the tissues. For this, triple-filtered matured paraffin with a melting point of 58-60°C was applied. The paraffin used in the L-mould to hold the organs was kept liquid while being allowed to solidify. Tissues were exposed for correct sectioning after the solid paraffin blocks were cut into little square blocks. A microtome (Medimeas, MRM-RM 1191) was used to cut the trimmed blocks into sections or ribbons, each 5 µmthick. Onto clean, lint-free glass slides were carefully transferred good parts. Mayer's albumin was added to the grease-free slides to help the tissues adhere to the slides more effectively. The slides with the necessary length ribbons were placed on a hot plate with warm water kept at 50-55 °C to stretch and flatten the wrinkled tissues. The dry slides were stained using hematoxylin and eosin double staining (H&E) procedures [7]. DPX (Dibutyl Phthalate Xylene) mountant was used to firmly attach slides to the slideshow. With the aid of the computer-attached microscope, the sections were screened. An advanced trinocular research microscope (Axioscope 2 Plus, Zeiss, Japan) attached to an Axio-Cam ICc 5 camera was used to take digital colour microphotographs of the chosen slides at various magnifications mounted to the microscope. The photos were taken using Zen 2 (Blue Edition).

Histopathological analyses and scoring

The degree of the histological alterations in the several organs of *P. hypophthalmus* treated with FFL was assessed in comparison to the control. The primary alterations were noted and given qualitative (numerical) values, as shown below, based on how much the tissue had changed because of damage to its natural architecture. The Bowker et al. [8] grading system was used as the foundation for histopathological scoring, which is detailed in Table 1.

Statistical analysis

The data were expressed as mean ± standard deviation. The qualitative scores were analyzed by non-parametric Kruskal Wallis test with pair-wise comparisons. The statistical analyses were done using Statistical Package for Social Sciences (IBM-SPSS), version 25.0, considering a probability level of $p<0.05$.

RESULTS AND DISCUSSION

Notable histoarchitectural anomalies in the tissues of *P. hypophthalmus* dosed with FFL at concentrations ranging from 0 to 10 times the minimum therapeutic dose of 10 mg kgbiomass^{-1} day^{-1} (×) for 30 consecutive days were observed. Tables 2A and 2B present the qualitative scores of the histopathological alterations in the kidney, liver, gill, and spleen sections in comparison with normal architecture.

Kidneys

On day 10 of FFL dosing, the kidneys of the 1× group exhibited significant degeneration of renal tubules, mild degeneration of tubular epithelium, vacuolation, hydropic swelling, mineralization, and necrotized renal interstitium. Similar changes were observed on day 20, albeit with increased severity. Although there was an insignificant increase ($p>0.05$) in renal tubular degeneration, other alterations were considered mild and insignificant ($p>0.05$) except for necrotized areas and renal interstitium, which peaked significantly ($p<0.05$). Likewise, on day 30, there was a significant ($p>0.05$) increase in the degeneration of renal tubules, mild hydropic swelling, vacuolation, and mineralization, along with a significantly increased ($p<0.05$) degeneration of renal tubular epithelium and thickened, widened lumen. Mildly necrotized areas also significantly increased ($p<0.05$) on day 30. However, after 10 days of cessation of dosing, *i.e.*, on day 10 post-FFL-dosing, there was a significant reduction ($p<0.05$) in histopathological abnormalities and recovery of renal tissues was observed, although mild degeneration of renal tubules persisted for a longer period with reduced intensity (Table 2A; Fig. 1a, 1e). The histological examination of the kidneys of *P. hypophthalmus* administered 3× dose revealed pronounced degeneration of renal tubules and mild degeneration of renal tubular epithelium, along with necrotized renal interstitium, hydropic swelling, vacuolation, and mineralization on day 10. Similar changes were observed on day 20, with a significant increase ($p<0.05$) in the degeneration of renal tubules, renal tubular epithelium, vacuolation, and necrotized

Table 1. The qualitative ordinal scale for assessing the degree of histopathological changes.

Histopathological change	Level
No change	0
Normal (<5% of tissues affected)	1
Mild (5-15% of tissues affected)	2
Moderate (15-25% of tissues affected)	3
Marked (25-50% of tissues affected)	4
Severe (>50% of tissues affected)	5

Table 2A. Qualitative assessment of the major histopathological changes in florfenicol (FFL)-dosed *Pangasianodon hypophthalmus* at 1 to 3 times the therapeutic dose of 10 mg kgbiomass-1day-1 for 30 consecutive days in comparison with normal architecture.

	Qualitative assessment on a five-point ordinal scale*							
	1×				3×			
	10FD	20FD	30FD	10PD	10FD	20FD	30FD	10PD
Kidney								
DG	3.06±0.08^{1ac}	3.04±0.08^{1ac}	3.11±0.09^{1ace}	1.59±0.37^{2b}	3.09±0.03^{1ace}	3.14±0.04^{1,2ce}	3.19±0.04^{2ce}	2.15±0.10^{3d}
DRE	1.12±0.13^{1a}	1.18±0.15^{1ag}	1.27±0.14^{2bg}	0.81±0.32^{3c}	1.57±0.12^{1d}	1.69±0.17^{1,2d}	1.74±0.10^{2df}	0.82±0.18^{3e}
HS	1.26±0.10^{1a}	1.41±0.11^{1ac}	1.43±0.13^{1ac}	0.81±0.34^{2b}	1.39±0.10^{1c}	1.42±0.10^{1ce}	1.54±0.10^{2ce}	0.98±0.07^{3d}
V	1.18±0.11^{1a}	1.19±0.17^{1a}	1.21±0.16^{1a}	0.79±0.18^{2b}	1.23±0.15^{1,3ad}	1.37±0.11^{1,2cd}	1.42±0.10^{2c}	1.22±0.08^{3a}
N	1.06±0.13^{1a}	1.31±0.14^{2b}	1.26±0.11^{3cg}	0.79±0.34^{4d}	1.07±0.12^{1b}	1.28±0.07^{2bc}	1.59±0.10^{3ef}	0.69±0.10^{4d}
M	1.11±0.15^{1a}	1.13±0.14^{1ac}	1.15±0.13^{1acd}	0.73±0.33^{2b}	1.42±0.16^{1cde}	1.36±0.14^{1de}	1.71±0.15^{1e}	1.13±0.12^{2f}
Liver								
CV	1.23±0.14^{1a}	1.35±0.10^{1,2ab}	1.41±0.10^{2b}	1.12±0.11^{1a}	1.35±0.08^{1a}	1.39±0.10^{2b}	1.41±0.07^{2b}	1.19±0.02^{1a}
CD	1.03±0.13^{1a}	1.07±0.08^{1abc}	1.07±0.09^{1ab}	1.04±0.08^{1ab}	1.13±0.06^{1abc}	1.15±0.08^{1bc}	1.16±0.10^{1cd}	1.12±0.03^{1bc}
CH	1.24±0.13^{1ac}	1.28±0.07^{1a}	1.29±0.10^{1a}	1.04±0.08^{2b}	1.24±0.16^{1acd}	1.30±0.06^{1ad}	1.39±0.11^{1ad}	1.19±0.03^{1c}
Gill								
EH	1.86±0.11^{1ag}	1.97±0.12^{1ag}	2.15±0.36^{2b}	1.47±0.28^{3c}	2.13±0.10^{1c}	2.28±0.10^{1bc}	2.61±0.10^{2d}	1.78±0.18^{3a}
C and ST	1.12±0.12^{1af}	1.17±0.12^{1af}	1.23±0.10^{1ac}	1.01±0.08^{2b}	1.15±0.10^{1acd}	1.31±0.11^{1cd}	1.38±0.10^{1cde}	1.08±0.08^{2b}
LH	1.13±0.15^{1af}	1.17±0.13^{1ac}	1.19±0.12^{1ac}	0.78±0.13^{2b}	1.19±0.11^{1ce}	1.24±0.13^{1ce}	1.28±0.12^{1ce}	0.92±0.23^{2d}
EF	0.65±0.16^{1a}	0.77±0.27^{1,2ab}	0.79±0.26^{2b}	0.64±0.29^{3c}	1.06±0.13^{1,3d}	1.14±0.07^{1,2de}	1.19±0.07^{2e}	0.99±0.23^{3f}
Spleen								
ISS	1.31±0.17^{1a}	1.68±0.10^{2b}	1.72±0.11^{2bd}	1.28±0.10^{3c}	1.52±0.15^{1a}	1.68±0.18^{2bd}	1.75±0.10^{3bd}	1.54±0.08^{1a}
SN	1.64±0.10^{1a}	1.95±0.10^{2b}	2.01±0.20^{2b}	1.83±0.10^{3c}	1.83±0.27^{1b}	1.97±0.22^{1,2b}	2.04±0.25^{2d}	1.91±0.09^{3c}

Table 2B. Qualitative assessment of the major histopathological changes in florfenicol (FFL)-dosed *Pangasianodon hypophthalmus* at 5 to10 times the therapeutic dose of 10 mg kgbiomass-1day-1 for 30 consecutive days in comparison with normal architecture.

	Qualitative assessment on a five-point ordinal scale*							
	5×				10×			
	10FD	20FD	30FD	10PD	10FD	20FD	30FD	10PD
Kidney								
DG	3.18±0.04^{1ce}	3.21±0.04^{1ce}	3.24±0.06^{1e}	2.63±0.12^{2f}	3.32±0.04^{1g}	3.31±0.05^{1g}	3.37±0.04^{1g}	2.12±0.13^{2f}
DRE	1.61±0.10^{1d}	1.79±0.10^{2f}	1.85±0.14^{2f}	1.21±0.07^{3g}	2.09±0.10^{1h}	2.13±0.07^{1,2hi}	2.22±0.10^{2i}	1.27±0.15^{3b}
HS	1.45±0.07^{1e}	1.47±0.10^{1e}	1.73±0.10^{2f}	1.13±0.10^{3g}	1.75±0.18^{1h}	1.94±0.10^{1h}	2.02±0.07^{2i}	1.32±0.17^{3j}
V	1.27±0.10^{1d}	1.39±0.10^{1d}	1.41±0.06^{1cd}	1.26±0.06^{2a}	1.72±0.10^{1e}	1.81±0.14^{2f}	1.86±0.13^{2f}	1.41±0.14^{3a}
N	1.31±0.10^{1b}	1.52±0.10^{2eg}	1.66±0.07^{3fh}	1.37±0.07^{2g}	1.52±0.27^{1h}	1.71±0.13^{1h}	1.89±0.10^{2i}	1.68±0.11^{1h}
M	1.28±0.07^{1e}	1.28±0.19^{1e}	1.59±0.10^{2g}	1.32±0.06^{3a}	1.89±0.10^{1g}	1.96±0.14^{1,2g}	2.19±0.10^{2g}	1.46±0.07^{3e}
Liver								
CV	1.22±0.11^{1a}	1.34±0.15^{2b}	1.39±0.12^{2b}	1.19±0.13^{1a}	1.21±0.10^{1a}	1.32±0.10^{2b}	1.36±0.11^{2b}	1.21±0.20^{1a}
CD	1.15±0.09^{1cd}	1.19±0.08^{1cd}	1.24±0.11^{1de}	1.11±0.15^{1cd}	1.26±0.11^{1,2ef}	1.35±0.12^{1f}	1.39±0.20^{1f}	1.17±0.24^{2cd}
CH	1.17±0.08^{1c}	1.31±0.10^{2de}	1.35±0.11^{2de}	1.22±0.11^{1ac}	1.25±0.10^{1acd}	1.32±0.08^{2de}	1.42±0.12^{2e}	1.20±0.16^{1ac}
Gill								
EH	2.47±0.14^{1d}	2.61±0.10^{2eh}	2.69±0.41^{3fh}	2.10±0.09^{4g}	2.63±0.11^{1de}	2.71±0.13^{2h}	2.86±0.07^{3i}	2.49±0.12^{4d}
C and ST	1.32±0.10^{1cde}	1.44±0.11^{1de}	1.51±0.10^{1e}	1.11±0.07^{2f}	2.53±0.30^{1g}	2.71±0.07^{2h}	2.93±0.07^{2i}	2.61±0.13^{1g}
LH	1.21±0.14^{1ce}	1.32±0.08^{1e}	1.35±0.12^{1e}	1.07±0.10^{2f}	1.71±0.11^{1g}	1.83±0.13^{2h}	1.96±0.16^{2i}	1.53±0.09^{1g}
EF	1.17±0.10^{1,2de}	1.24±0.08^{1de}	1.32±0.10^{1g}	1.07±0.23^{2h}	1.19±0.13^{1e}	1.32±0.10^{2g}	1.49±0.14^{3i}	1.27±0.11^{2g}
Spleen								
ISS	1.61±0.17^{1a}	1.74±0.12^{2bd}	1.82±0.16^{2bd}	1.58±0.14^{1a}	1.71±0.10^{1d}	1.94±0.17^{2fe}	2.06±0.11^{3f}	1.98±0.08^{2g}
SN	2.10±0.19^{1bd}	2.17±0.21^{2d}	2.26±0.16^{2e}	1.82±0.08^{3c}	2.14±0.20^{1d}	2.29±0.24^{2e}	2.43±0.12^{3f}	2.15±0.04^{1g}

[*Qualitative assessment ordinal scale: 0 = No change; 1 = Normal with <5% tissues affected; 2 = Mild with 5-15% tissues affected; 3 = Moderate with 15-25% tissues affected; 4 = Marked with 25-50% tissues affected and 5 = Severe with >50% tissues affected. Qualitative assessment was based on six observations(mean±standard deviation) for each organ of the respective group. No changes were noted in the control group. 1-4: Values sharing a common numerical superscript within a row for a particular histopathological change for a particular treatment (dose) differed insignificantly (p>0.05). a-j: Values sharing a common alphabetical superscript for a particular row among the treatments (doses) differed insignificantly (p>0.05). 10FD: Day 10 FFL-dosing; 20FD: Day 20 FFL-dosing; 30FD: Day 30 FFL-dosing; 10PD: Day 10 post-FFL-dosing. DG: Degeneration of renal tubules; DRE: Degeneration of renal tubular epithelium; HS: Hydropic swelling; V: Vacuolation; N: Necrotized renal tubule; M: Mineralization; CV: Cytoplasmic vacuolation; CD: Cytoplasmic degeneration; CH: Cellular hypertrophy; EH: Epithelial hyperplasia; C: Curling of secondary lamellae; ST: Swollen tips of secondary lamellae; LH: Secondary lamellar hyperplasia; EF: Erosion of secondary lamellae; ISS: Increased sinusoidal space; SN: Splenic necrosis].

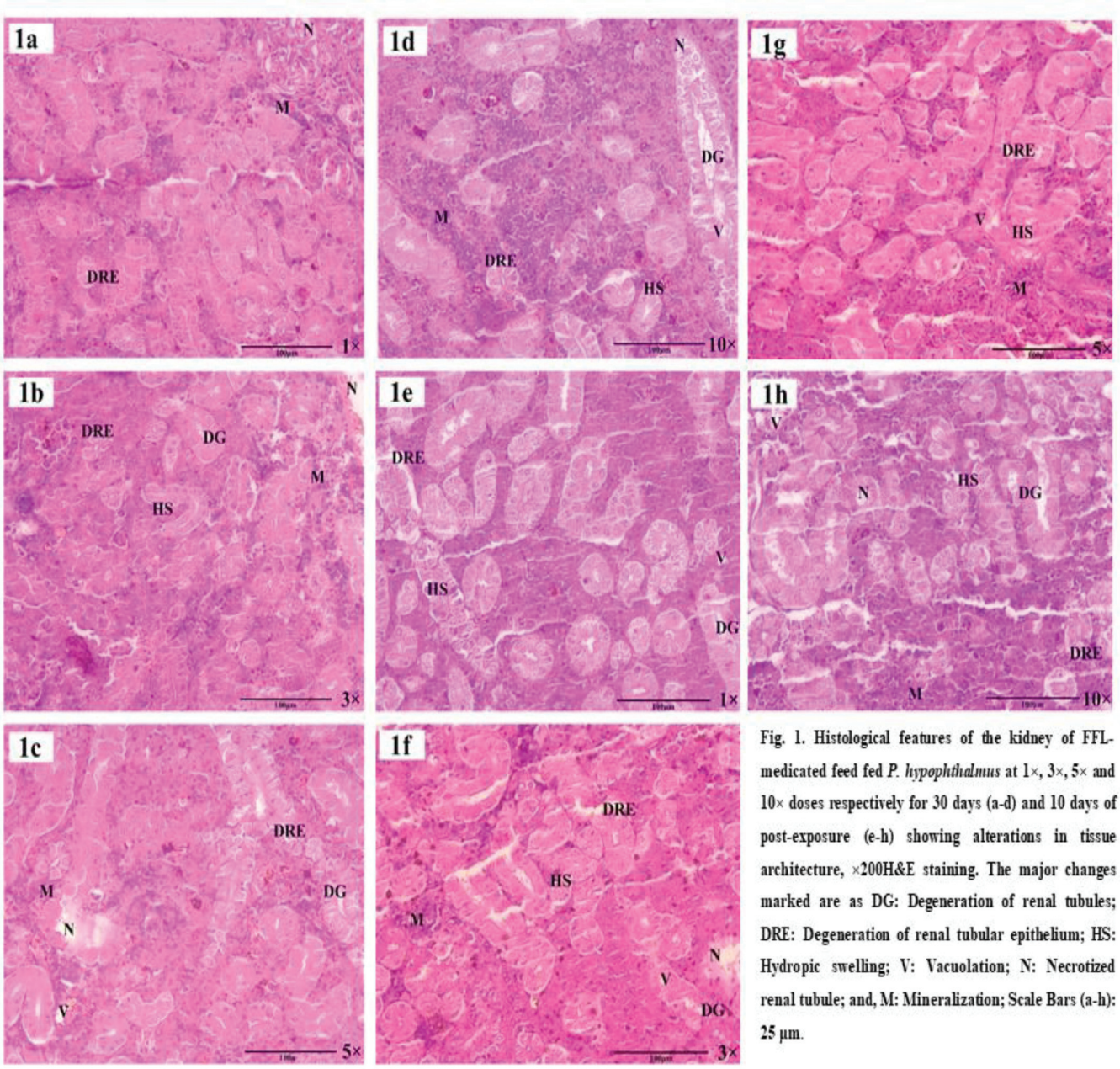

Fig. 1. Histological features of the kidney of FFL-medicated feed fed *P. hypophthalmus* at 1×, 3×, 5× and 10× doses respectively for 30 days (a-d) and 10 days of post-exposure (e-h) showing alterations in tissue architecture, ×200H&E staining. The major changes marked are as DG: Degeneration of renal tubules; DRE: Degeneration of renal tubular epithelium; HS: Hydropic swelling; V: Vacuolation; N: Necrotized renal tubule; and, M: Mineralization; Scale Bars (a-h): 25 µm.

renal interstitium. There was a significant increase ($p>0.05$) in hydropic swelling. On the 30th day of dosing, there was an insignificant increase ($p>0.05$) in the degeneration of renal tubules, hydropic swelling, vacuolation, mineralization, and degeneration of renal tubular epithelium, along with a significant increase ($p<0.05$) in necrotized areas and widening of the lumen with proteinaceous cast, inflammation, and necrotized hematopoietic tissues. On day 10 post-FFL-dosing, there was a significant reduction ($p<0.05$) in histopathological abnormalities in the 3×group, although some degenerated renal tubules, vacuolation, hydropic swelling, and thickened and widened lumens persisted. The scores for degenerated renal epithelium, necrotized areas, and mineralization were within normal limits [Table 2A; Fig. 1(b, f)].

The 5×group's kidney sections exhibited marked degeneration of renal tubules and mild degeneration of tubular epithelium, along with necrotized areas, hydropic swelling, inflamed renal tubules, vacuolation, and mineralization after 10 days. By day 20, there was a significant increase ($p<0.05$) in the degeneration of tubular epithelium and necrotized areas. Similarly, on day 30, there was a significant increase ($p<0.05$) in

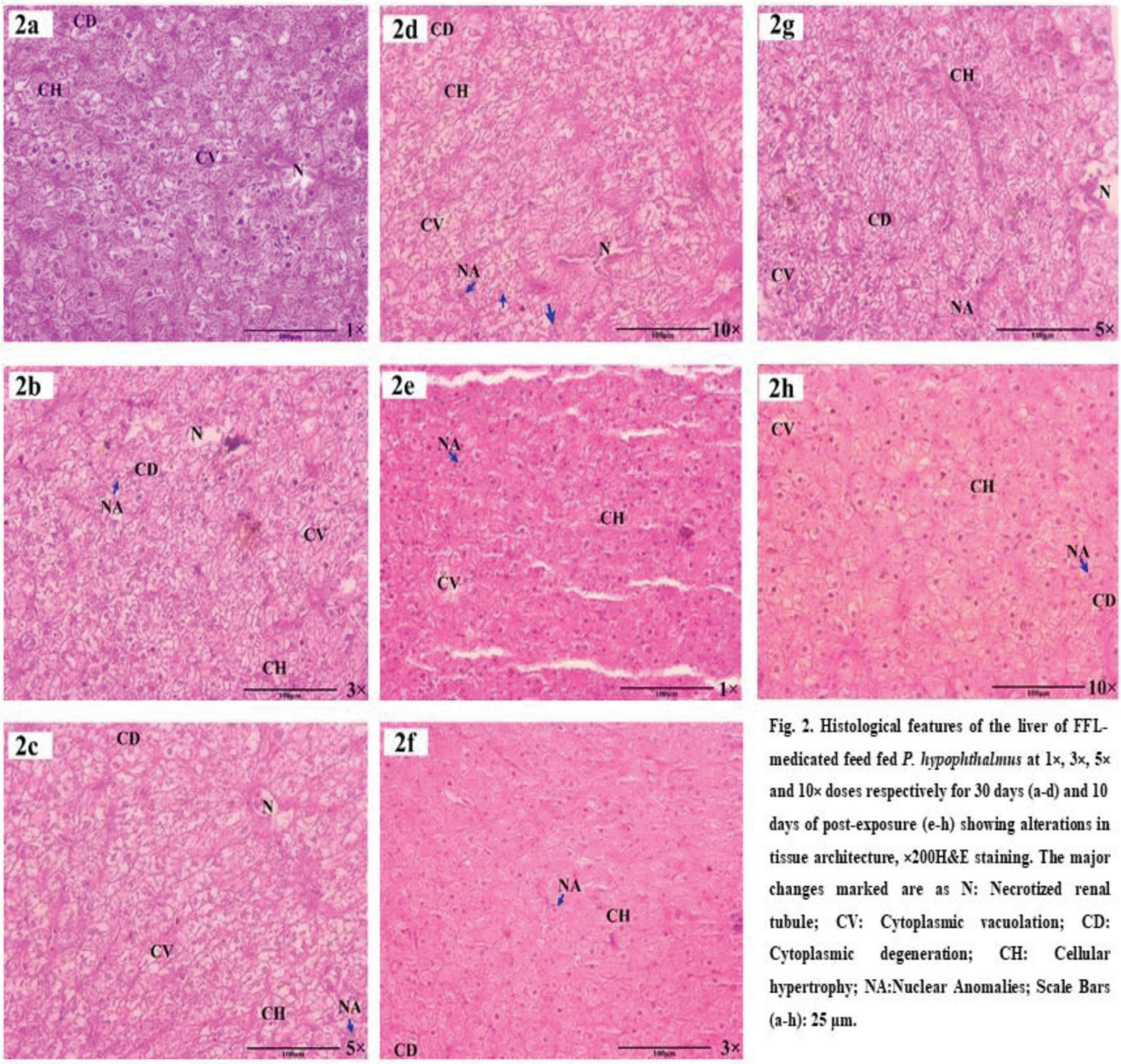

Fig. 2. Histological features of the liver of FFL-medicated feed fed *P. hypophthalmus* at 1×, 3×, 5× and 10× doses respectively for 30 days (a-d) and 10 days of post-exposure (e-h) showing alterations in tissue architecture, ×200H&E staining. The major changes marked are as N: Necrotized renal tubule; CV: Cytoplasmic vacuolation; CD: Cytoplasmic degeneration; CH: Cellular hypertrophy; NA:Nuclear Anomalies; Scale Bars (a-h): 25 µm.

the alterations like degeneration of tubular epithelium, hydropic swelling, mineralization, and necrotized areas, with an insignificant increase in tubular degeneration and vacuolation. On day 10 post-dosing, there was a significant reduction ($p<0.05$) in kidney tissue abnormalities, although mild necrotized areas, mineralization, widened and thickened lumens, and inflamed and moderately degenerated renal tubules persisted (Table 2B; Figs. 1c, 1g).In the 10× group, after 10 days of dosing, kidney sections showed marked degeneration of renal tubules and moderately degenerated tubular epithelium, along with mild necrotized areas, hydropic swelling, widened and thickened lumens, inflamed renal tubules, vacuolation, and mineralization. By day 20, there was a significant increase ($p<0.05$) in the degeneration of tubular epithelium, vacuolation, and mineralization, along with degeneration of renal tubules, hydropic swelling, and necrotized areas, albeit insignificant ($p>0.05$). On day 30, there was an insignificant increase ($p>0.05$) in the degenerated tubular epithelium, degeneration of renal tubules, vacuolation, and mineralization, followed by a significant increase ($p<0.05$) in necrotized areas and hydropic swelling. However, on day 10 post-dosing,

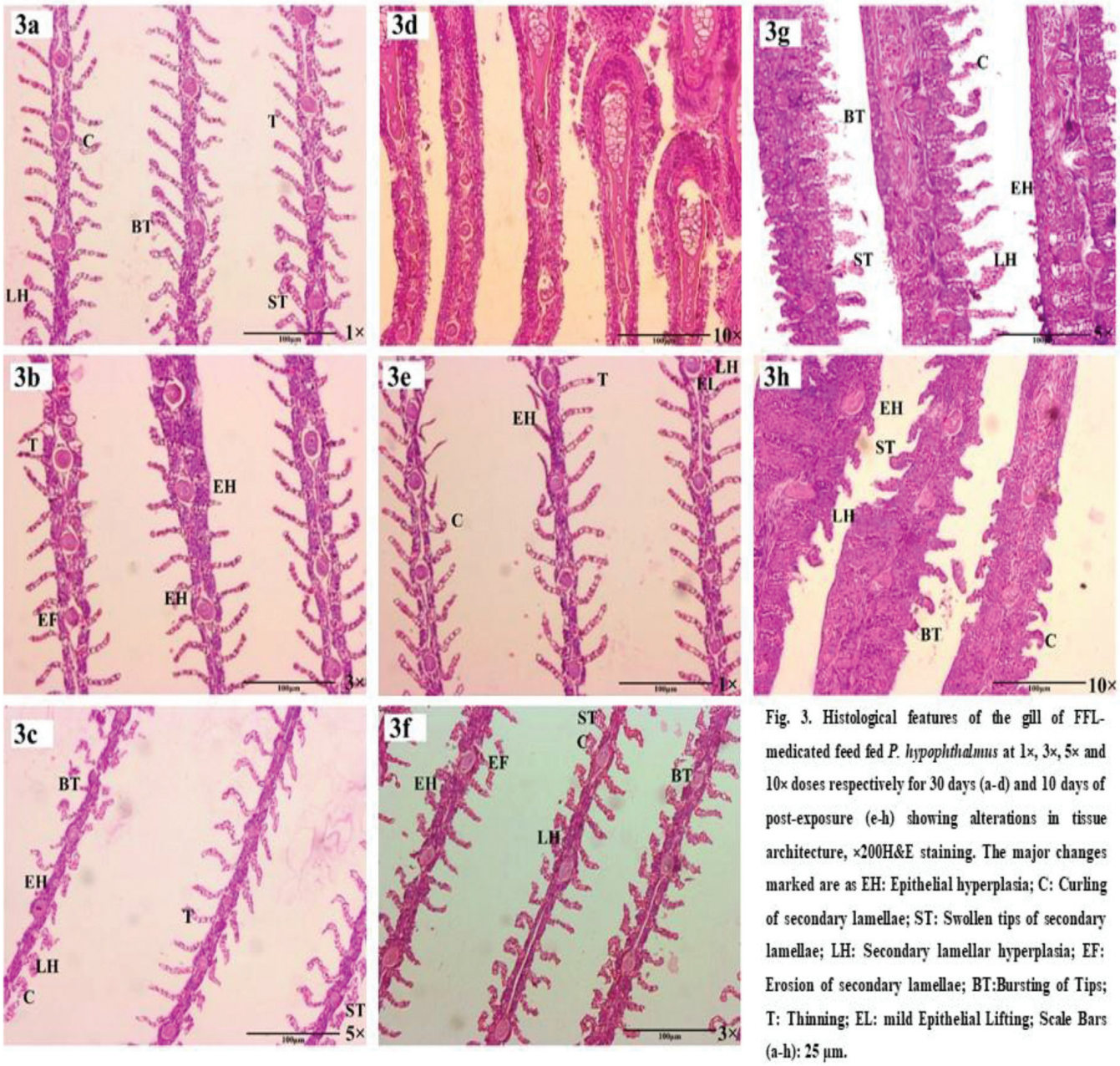

Fig. 3. Histological features of the gill of FFL-medicated feed fed *P. hypophthalmus* at 1×, 3×, 5× and 10× doses respectively for 30 days (a-d) and 10 days of post-exposure (e-h) showing alterations in tissue architecture, ×200H&E staining. The major changes marked are as EH: Epithelial hyperplasia; C: Curling of secondary lamellae; ST: Swollen tips of secondary lamellae; LH: Secondary lamellar hyperplasia; EF: Erosion of secondary lamellae; BT:Bursting of Tips; T: Thinning; EL: mild Epithelial Lifting; Scale Bars (a-h): 25 µm.

there was a significant reduction ($p<0.05$) in kidney tissue abnormalities, although some necrotized hematopoietic tissues, necrotized areas, widened and thickened lumens, inflamed renal tubules, and degeneration of renal tubules persisted [Table 2B; Fig. 1(d, h)].

Liver

On the 10th day of FFL administration, the 1× group exhibited mild cytoplasmic vacuolation, cytoplasmic degeneration, and cellular hypertrophy in hepatic cells. By day 20, there was a slight increase ($p>0.05$) in histological abnormalities such as mild cytoplasmic degeneration, along with hepatic nuclear abnormalities and dilated hepatic cords, primarily featuring bi-nucleated hepatocytes. By day 30, there was a further but insignificant increase in aberrations including cytoplasmic vacuolation, degeneration, cellular hypertrophy, dilated hepatic cords, and various nuclear anomalies in hepatocytes, along with a reduction in nuclear numbers. After 10 days of dose termination, significant recovery was observed in the 1× liver tissue, with mild cytoplasmic vacuolation and cellular hypertrophy, and a reduction in cytoplasmic degeneration [Table 2A; Fig. 2(a, e)]. In the 3× group, liver tissues showed similar trends with mild

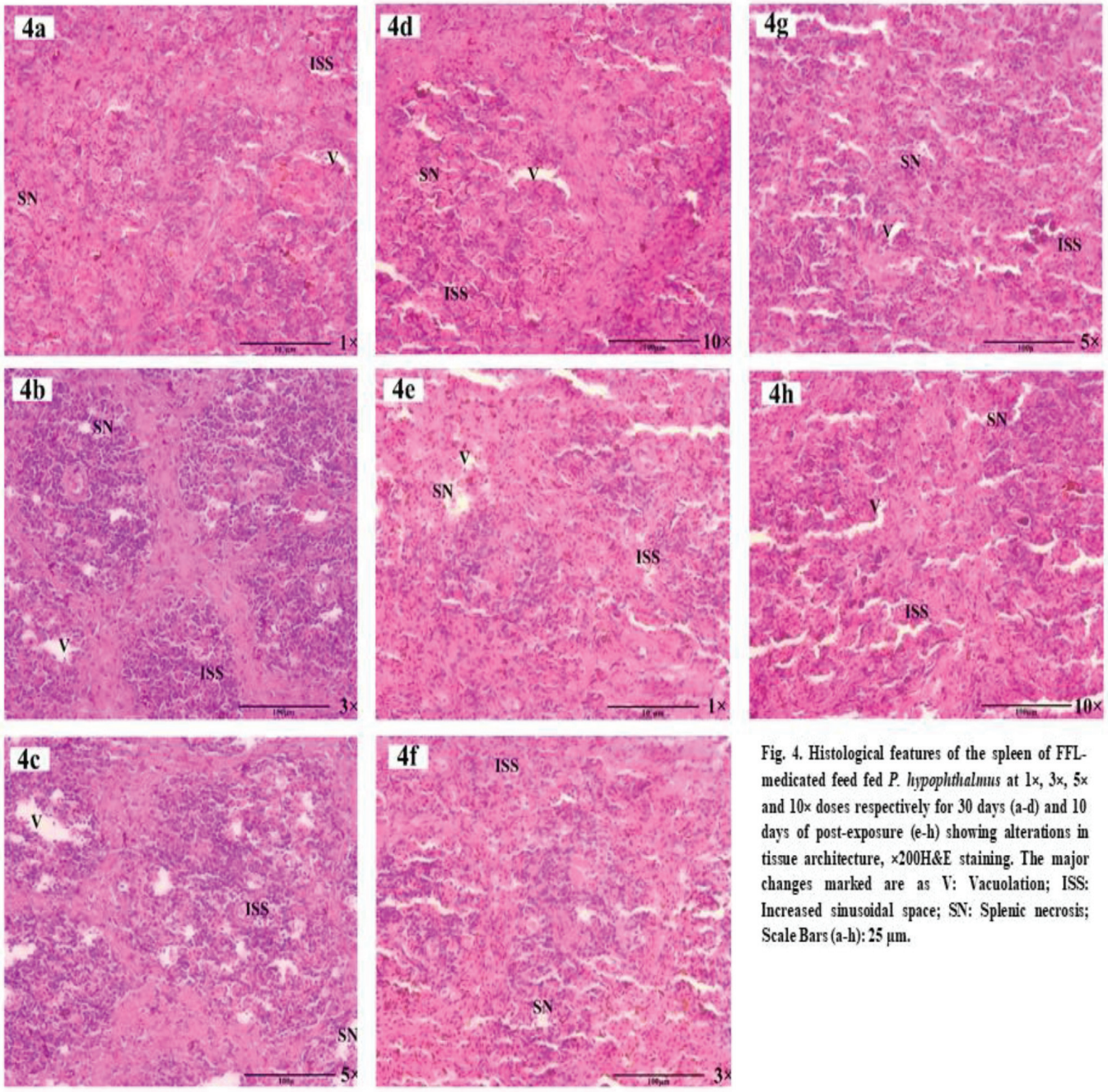

Fig. 4. Histological features of the spleen of FFL-medicated feed fed *P. hypophthalmus* at 1×, 3×, 5× and 10× doses respectively for 30 days (a-d) and 10 days of post-exposure (e-h) showing alterations in tissue architecture, ×200H&E staining. The major changes marked are as V: Vacuolation; ISS: Increased sinusoidal space; SN: Splenic necrosis; Scale Bars (a-h): 25 µm.

cytoplasmic vacuolation, degeneration, and hepatocyte nuclear abnormalities on day 10, although the rate of change compared to the 1× group was insignificant ($p>0.05$). By day 20 and 30, the alterations persisted with similar patterns, including cytoplasmic degeneration, cellular hypertrophy, cytoplasmic vacuolation, reduction in hepatic nuclei, and congregation of nuclei towards hepatic cords. After 10 days of dose termination, significant recovery occurred in the 3× liver tissues, though cytoplasmic degeneration and cellular hypertrophy remained insignificantly reduced ($p>0.05$), while cytoplasmic vacuolation was still evident [Table 2A; Fig. 2(b, f)]. In the 5× group, liver tissues displayed mild cytoplasmic vacuolation, degeneration, and cellular hypertrophy along with hepatocyte nuclear abnormalities on day 10. By day 20, there was a significant increase in cytoplasmic vacuolation and cellular hypertrophy, along with an insignificant increase in cytoplasmic degeneration, and an increased occurrence of degenerated or karyolytic hepatocyte nuclei. By day 30, a reduction in hepatocyte nuclei numbers was noted, alongside continued

cytoplasmic vacuolation and cellular hypertrophy. With dose termination, there was an insignificant reduction in these abnormalities, with hepatocyte nuclear anomalies persisting [Table 2B; Fig. 2(c, g)]. In the 10× group, almost similar observations were made on days 10 and 20 of dosing, with an insignificant increase in the intensity of cytoplasmic vacuolation and cellular hypertrophy, and a significant increase in cytoplasmic degeneration by day 20. By day 30, an insignificant increase in all the anomalies was observed. With the suspension of dosing, there was a mild yet significant reduction in cytoplasmic vacuolation, although cytoplasmic degeneration persisted [Table 2B; Fig. 2(d, h)].

Gills

In the 1× group, on day 10, there was mild epithelial hyperplasia and thinning, along with curling of secondary lamellae. These effects slightly intensified insignificantly ($p>0.05$) by day 20, with increased epithelial lifting despite nearly mild scores. By day 30, there was a significant increase ($p<0.05$) in epithelial hyperplasia and secondary lamellar curling, while the swollen tips showed insignificant alterations ($p>0.05$). After a 10-day cessation of dosing, there was a significant reduction ($p<0.05$) in tissue aberrations, with persistent epithelial hyperplasia and secondary lamellar curling in the 1× group (Table 2A; Figs. 3a, 3e).In the 3× group, on day 10, there was moderate epithelial hyperplasia, mild secondary lamellar hyperplasia, and swelling of tips, along with thinning and erosion of secondary lamellae. Changes slightly intensified insignificantly ($p>0.05$) by day 20. A significant increase ($p<0.05$) in epithelial hyperplasia and secondary lamellar hyperplasia was observed by day 30, along with persistent curling and swollen tips. After a 10-day cessation of dosing, there was a significant reduction ($p<0.05$) in tissue aberrations, with persistent epithelial hyperplasia and eroded secondary lamellae in the 3× group (Table 1; Figs. 3b, 3f). In the 5× group, on day 10, there was moderate epithelial hyperplasia, mild secondary lamellar hyperplasia, and swollen tips. By day 20, there was a significant increase ($p<0.05$) in epithelial hyperplasia, while changes in secondary lamellar hyperplasia and swollen tips were insignificant. By day 30, there was a significant deterioration ($p<0.05$) in tissue architecture, with a significant increase in epithelial hyperplasia and curling and swollen tips, along with erosion of secondary lamellae. After cessation of treatment, there was a significant recovery ($p<0.05$), although epithelial hyperplasia and secondary lamellar alterations persisted (Table 2B; Fig. 3c, 3g). In the 10× group, on day 10, moderately high epithelial hyperplasia and swelling and bursting of tips of secondary lamellae were noted. By day 20, alterations significantly increased ($p<0.05$), with marked curling and erosion of secondary lamellae, along with epithelial and secondary lamellar hyperplasia. By day 30, there was further deterioration in secondary lamellar architecture, with marked curling and oedema, although changes compared to day 20 were insignificant ($p>0.05$). However, the increase ($p<0.05$) in epithelial hyperplasia, erosion, and thinning were significant. After cessation of dosing, there was a scanty yet significant ($p<0.05$) recovery, although epithelial hyperplasia and secondary lamellar alterations persisted [Table 2B; Fig. 3(d, h)].

Spleen

The spleen tissues of FFL-administered *P. hypophthalmus* exhibited alterations such as increased sinusoidal space, necrosis, and vacuolation in a dose-dependent manner. The 1×group's spleens on day 10 showed moderate splenic necrosis, mild vacuolation, and a slight increase in sinusoidal space, all of which significantly intensified ($p<0.05$) by day 20. By day 30, there was a further, albeit insignificant ($p>0.05$), increase in sinusoidal space, vacuolation, and splenic necrosis. However, after 10 days of dose termination, there was considerable recovery, with a significant reduction ($p<0.05$) in alterations, though increased sinusoidal space, vacuolation, and splenic necrosis persisted (Table 2A; Figs. 4a, 4e). In the 3× dosage group, on day 10, there was moderate splenic necrosis, a mild increase in sinusoidal space, and vacuolation. By day 20, there was an insignificant increase ($p>0.05$) in splenic necrosis but a significant increase ($p<0.05$) in sinusoidal space and vacuolation. Day 30 showed moderate splenic necrosis, increased sinusoidal space, and marked vacuolation, although the increase was insignificant ($p>0.05$). After 10 days of dose termination, there was a mild but significant ($p<0.05$) recovery of splenic tissues, with persistent splenic necrosis, increased sinusoidal space, and vacuolation (Table 2A; Fig. 4b, 4f).In the 5×group, on day 10, a significant increase ($p<0.05$) in sinusoidal space, vacuolation, and splenic necrosis was noted. By day 20, there was an insignificant increase ($p>0.05$) in vacuolation and sinusoidal space, with persistent splenic necrosis. Day 30 showed a further insignificant increase ($p>0.05$). The dose suspension led to a significant reduction ($p<0.05$) in splenic necrosis, though increased

sinusoidal space and vacuolation persisted (Table 2B; Fig. 4c, 4g). At the 10× dosage level, on day 10, there was moderate splenic necrosis and a considerable increase in sinusoidal space and vacuolation. By day 20, similar changes were observed, with significantly higher ($p<0.05$) intensities of splenic necrosis and increased sinusoidal space. Day 30 showed a further significant increase ($p<0.05$) in splenic necrosis, vacuolation, and sinusoidal space. After 10 days of dose cessation, there was a meagre but significant ($p<0.05$) recovery, with persistent splenic necrosis, increased sinusoidal space, and vacuolation [Table 2B; Fig. 4(d, h)].

The findings of this study offer valuable insights into how FFL impacts various tissues of commercially important catfish, *P. hypophthalmus*. By conducting thorough histological examinations of key organs and tissues, the study revealed the effects of FFL on the structural integrity of this species. The discussion will delve into interpreting these findings in the context of aquaculture practices, evaluating potential health risks, and proposing strategies for responsible antibiotic use. The kidneys and liver, are often recognized as the primary targets of drug-induced toxicity [9]. Thus far, reports on the negative effects of FFL on fish kidney and liver tissues in tropical conditions have been scarce [10]. The notable degeneration of renal tubules in FFL-treated fish is similar to findings by Gaikowski *et al.* [11] suggesting toxic damage. The persistence of renal tubular degeneration, even after 40 days of FFL discontinuation, suggests potential tissue necrosis at therapeutic doses [12]. The widened lumen of the 1× group indicates excessive elimination rates, while manifestations of renal tubule hydropic swelling with intact nuclei support previous research. After metabolic conversion to FFA, FFL is mostly removed by the kidneys through glomerular filtration [13]. Despite extensive study, the mechanism causing damage to tubular cells and the onset of acute renal insufficiency remains unclear. However, it is hypothesized that FFA, enters tubular cells, disrupting crucial metabolic pathways. In our study, necrosis primarily affected interstitial tissues, while profound degeneration occurred in renal tubules, where drug absorption occurs [4]. Tubular degeneration may result in lysosomal leakage from tubular cells due to oxidative damage, increasing the risk of renal toxicity, vasoconstriction, and decreased renal blood flow [14]. FFL's lipophilic nature makes it conducive to inducing oxidative and iontophoretic damage, which can lead to mineralization within renal tissues [11]. Upon dosage cessation, the widening of the lumen in the 1× group suggested filtration flow difficulties and poor glomerulus function, potentially due to lingering FFA residues [4]. Considering the kidneys' crucial role in maintaining osmoregulatory balance and eliminating metabolic waste, such histopathological changes could disrupt the physiological equilibrium of *P. hypophthalmus*, potentially leading to renal dysfunction.

As indicated by increased liver cell space, extensive cellular vacuolation was notably observed in FFL-dosed groups, similar to earlier studies [8, 13]. Increased hepatocyte vacuolation, possibly dosage-related, signified a degenerative process causing metabolic injury and alterations in cell membrane integrity. The intense vacuolation resulted in the clustering of nuclei towards hepatic sinusoids, potentially enhancing cellular detoxification and oxygen uptake [15]. The presence of hepatocytes devoid of nuclei indicated severe FFL-induced hepatotoxicity. In contrast, the liver tissues of FFL-dosed fish in a previous study lacked abnormalities [12]. Despite primarily inhibiting bacterial ribosomal protein synthesis, FFL has been shown to inhibit various cellular processes, compromising the normal functioning of gills, and threatening ionic homeostasis and enzymatic activities [13]. Overall, considerable reductions in liver and kidney histological abnormalities at therapeutic levels within 10 days of dose suspension suggested ideal recovery and FFL tolerability in *P. hypophthalmus*. These findings supported prior research indicating fish liver susceptibility to antibiotic-induced harm and stressed the importance of prudent antibiotic usage in aquaculture to mitigate hepatic issues [1].

Alterations in the gills, such as epithelial hypertrophy, lamellar fusion, and mucous cell hyperplasia, indicated integrity and potentially compromised respiratory function [16, 17]. The gills are pivotal for gas exchange and ion regulation in fish and any disruption to their structure can impede oxygen uptake and ion regulation, thus affecting overall respiratory efficiency and osmo-regulation [17]. The observed epithelial hyperplasia of the gills, a direct protective response, was the most notable abnormality documented. Extended FFL administration led to moderate epithelial hyperplasia in the 1× group and nearly severe damage in the 10× group after 30 days of continuous feeding. The progressive changes were more pronounced and frequent after extended dosing, although similar changes were observed in the therapeutic dose group. Therefore, these alterations

can be considered common protective responses against dietary FFL. Epithelial and secondary lamellar hyperplasia observed here may result from the appearance of defense cells as part of a compensatory tissue repair mechanism. Increased operculum movement or breathing rates as an adaptation to extended FFL dosing could have increased blood flow to the filaments, resulting in swollen tips accompanied by an inflammatory response. The curling and swelling of secondary lamellae during extended administration suggested impaired oxygen uptake and anoxia. The swelling of secondary lamellar filaments indicated decreased efficiency of oxygen consumption [11].

In this study, fish administered extended FFL dosing exhibited noticeable changes in spleen tissue. Relevant histopathological alterations included dose-dependent splenic necrosis and increased sinusoidal space. The extent of splenic damage was moderate in the higher-dosed groups. Sinusoids in the spleen play roles in removing damaged erythrocytes and facilitating leukocyte migration. Increased sinusoidal space is often associated with various toxicants and pharmaceuticals. The dilated sinusoidal space observed in this study could be attributed to extend FFL dosing. However, the extent of splenic necrosis was moderate in the higher-dosed groups, indicating compromised blood flow and tissue ischemia [18, 19]. The ruptured erythrocytes and hemosiderin deposits in higher-dosed groups aligned with earlier studies, suggesting vascular damage due to FFL administration [20].

CONCLUSION

Florfenicol, a congener of toxic chloramphenicol, is legally permitted to be used in aquaculture practices in several countries. This research highlights the significance of understanding the histopathological effects of dietary FFL on commercially important catfish, *P. hypophthalmus*. The results of the present study showed multi-organ toxicity of the antibiotic, even at the recommended dose, in *P. hypophthalmus* highlighting the need for careful monitoring of fish under treatment or search for a safer antimicrobial for the treatment of bacterial infections in the catfish. Furthermore, our findings contribute to the advancement of sustainable aquaculture practices aimed at preserving fish health and environmental integrity. Based on these findings, it is crucial to take preventive actions to reduce the negative impacts of FFL on fish health and environmental well-being. This entails implementing rigorous antibiotic stewardship measures, including optimizing dosages, limiting treatment durations, and exploring alternative disease management strategies such as vaccination and probiotics.

REFERENCES

1. Manna SK, Bera AK, Das N *et al.* Determination of biosafety of the antibiotic oxytetracycline hydrochloride in *Pangasianodon hypophthalmus*. Aquac Res. 2021; 52: 2470-2480.

2. Bojarski B, Kot B, Witeska M. Antibacterials in aquatic environment and their toxicity to fish. Pharmaceuticals. 2020; 13: 189.

3. Rohani MF. Pesticides toxicity in fish: Histopathological and hemato-biochemical aspects-A review. Emerg Contam. 2023; 9: 100234.

4. Gaikowski MP, Mushtaq M, Cassidy P *et al.* Depletion of florfenicol amine, marker residue of florfenicol, from the edible fillet of tilapia (*Oreochromis niloticus* x *O. niloticus* and *O. niloticus* x *O. aureus*) following florfenicol administration in feed. Aquaculture. 2010; 301(1-4): 1-6.

5. Naylor RL, Hardy RW, Buschmann AH *et al.* A 20-year retrospective review of global aquaculture. Nature. 2021; 591(7851): 551-563.

6. USFDA. Approved aquaculture drugs. US Food and Drug Administration. 2022. Retrieved from https://www.fda.gov/animal-veterinary/aquaculture/approved-aquaculture-drugs.

7. Roberts RJ. Fish Pathology. John Wiley & Sons; 2012.

8. Bowker JD, Carty D, Bowman MP. The safety of Aquaflor (50% florfenicol) administered in feed to fingerling yellow perch. N Am J Aquac. 2013; 75: 517-523.

9. Gaikowski MP, Wolf JC, Endris RG *et al.* Safety of Aquaflor (florfenicol, 50% type A medicated article), administered in feed to channel catfish, *Ictalurus punctatus*. Toxicol Pathol. 2003; 31: 689-697.

10. Limbu SM, Chen L, Zhang M *et al.* A global analysis on the systemic effects of antibiotics in cultured fish and their potential human health risk: a review. Rev Aquacult. 2020; 13: 1015-1059.

11. Gaikowski MP, Wolf JC, Schleis SM *et al.* Safety of florfenicol administered in feed to tilapia (*Oreochromis* sp.). Toxicol Pathol. 2012; 41: 639-652.

12. Straus DL, Bowker JD, Bowman MP *et al.* Safety of aquaflor-medicated feed to sunshine bass. N Am J Aquac. 2012; 74(1): 1-7.

13. Bardhan A, Abraham TJ, Singha J *et al.* Histopathological aberrations and oxidative stress responses in Nile tilapia *Oreochromis niloticus* as influenced by dietary florfenicol and its metabolites. Aquaculture. 2022; 559: 738447.

14. Seely JC, Francke S, Mog SR *et al.* Renal papillary rarefaction: An artifact mimicking papillary necrosis. Toxicol Pathol. 2019; 47(5): 645-648.

15. Shiroma LS, Soares MP, Cardoso IL *et al.* Evaluation of health and environmental risks for juvenile tilapia (*Oreochromis niloticus*) exposed to florfenicol. Heliyon 2020; 6: e05716.

16. Ahmed MdK, Habibullah-Al-Mamun Md, Parvin E *et al.* Arsenic induced toxicity and histopathological changes in gill and liver tissue of freshwater fish, tilapia (*Oreochromis mossambicus*). Exp Toxicol Pathol. 2013; 65: 903-909.

17. Rodrigues S, Antunes SC, Nunes B *et al.* Histopathological effects in gills and liver of *Sparus aurata* following acute and chronic exposures to erythromycin and oxytetracycline. Environ Sci Pollut Res. 2019; 26: 15481-15495.

18. Sales CF, Silva RF, Amaral MGC *et al.* Comparative histology in the liver and spleen of three species of freshwater teleost. Neotrop Ichthyol. 30; 15: e160041.

19. Khan Z, Chetty R. A review of the cysts of the spleen. Diagn Histopathol. 2016; 22: 479-484.

20. Rodrigues RA, do Nascimento Silva AL, Siqueira MS *et al.* Hematological, biochemical, and histopathological responses in sorubim *Pseudoplatystoma* spp. experimentally infected with *Lactococcus garvieae*. Aquac Int. 2020; 28: 1907-1923.

Cite this article as: Das N, Abraham TJ, Bera AK, Manna SK, Sen A, Chatterjee S. Histoarchitectural anomalies induced by antibiotic florfenicol in commercially important catfish *Pangasianodon hypophthalmus*. Explor Anim Med Res. 2024; 14(1), DOI: 10.52635/eamr/14.1.112-123.